



Comparison of low-pressure oxygen plasma and chemical treatments for surface modifications of Ti6Al4V

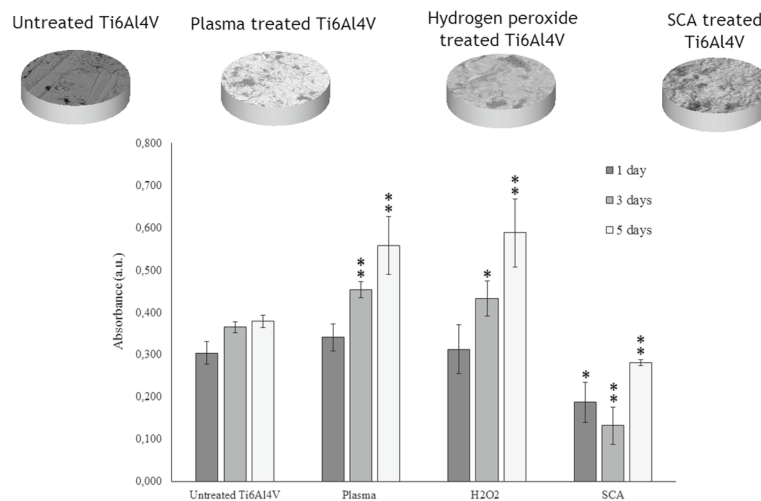
María Elena Alemán-Domínguez¹ · Zaida Ortega¹ · Antonio N. Benítez¹ · Aday Romero-Pérez² · Ling Wang³ · Ruymán Santana-Farré² · Francisco Rodríguez-Esparragón⁴

Received: 18 January 2019 / Accepted: 11 February 2019 / Published online: 9 March 2019
© Zhejiang University Press 2019

Abstract

Different treatments were conducted over Ti6Al4V samples in order to produce a surface modification to increase cell attachment and proliferation. The surface treatments evaluated in this study were as follows: etching with sulfuric acid/hydrochloric acid, oxidizing with hydrogen peroxide and low-pressure oxygen plasma treatment. In contrast to other works found in the literature, this research conducts a comparison between different chemical and physical treatments in terms of different assays for surface characterization: X-ray diffraction, scanning electron microscope (SEM), energy-dispersive X-ray spectroscopy, water contact angle, release of vanadium ions and cell viability tests (MTT) of human osteoblasts (hFOB 1.19). Cell morphology over the different substrates was also studied by SEM observation. It was found that plasma and peroxide treatments increase the O/Ti ratio at the titanium surface and provide an increase in cell affinity. On the other hand, acid etching provides a superhydrophilic surface which is not able to improve the cell attachment of human osteoblasts.

Graphical abstract



Keywords Surface activation · Titanium alloys · Surface functionalization · Low-pressure plasma

Electronic supplementary material The online version of this article (<https://doi.org/10.1007/s42242-019-00036-9>) contains supplementary material, which is available to authorized users.

✉ Zaida Ortega
zaida.ortega@ulpgc.es

Extended author information available on the last page of the article

Introduction

The increase in life expectancy also implies an increase in the number of patients suffering from degenerative pathologies such as osteoarthritis. Titanium alloy implants are widely used as substitutes for the natural bone in bone,

both in bone and as part of dental implants [1]. Studies conducted by different authors show that the recurring failures in implants can be attributed to the lack of bone and its bad quality and that implants currently used cannot ensure stability, functionality and durability, even when the natural bone is not broken [2, 3].

Titanium and its alloys are biocompatible but also bioinert, which means that it will not interact with the surrounding tissues and, thus, will not promote cells adhesion and proliferation, leading to a limited osseointegration of implants in the natural bone [4, 5]. To increase cell attachment to titanium alloys other authors have conducted topographical modifications [6–9] or chemical changes to introduce bioactive substances, both of inorganic (such as calcium phosphates or hydroxyapatite) [10–13] or of organic nature (such as polymers, proteins or polysaccharides) [14–19]. Regarding physical methods, Ramskogler and collaborators [9] propose the use of a highly energetic electron beam structuring over Ti surfaces; this technique is said to produce a surface free of cracks, pores and impurities, also leading to an improvement in cell proliferation. According to these and other researchers, the effect of surface topography on bone integration is unclear and difficult to measure. Some authors have grafted poly(sodium styrene sulfonate) over Ti substrates to later attach proteins (albumin, fibronectin and collagen I), proving an effective grafting of poly(NaSS) over the titanium surface and an enhanced cell growth and dispersion [16, 19]; besides, *in vivo* studies show the presence of mineralized tissues adjacent to the implant and no bacteria adhesion, that is, that the grafted surface is favorable to osseointegration and inhibits bacterial infection. Other interesting effects derived from the anchorage of polysaccharides to titanium alloys surfaces are the antibacterial activity of these coatings, especially for those made of chitosan/alginate and minocycline [20] or chitosan and lauric acid [5], together with the higher cell adhesion. This is remarkable because bacterial infection has been demonstrated to be the second cause of instability of titanium implants [4].

Although the above-mentioned introduction of bioactive substances have been proved to increase the bioaffinity of titanium parts, these methods are complex and expensive when they are intended to be used on commercial titanium prosthesis and implants. For this reason, simpler treatments which have a significant effect on the osseointegration of titanium parts are more promising for their massive clinical introduction. Examples of these kinds of treatments are ultraviolet [21, 22] or plasma exposure [23–25] of the surfaces. These procedures have been demonstrated to change the hydrophilicity of their surface without altering its topography [25]. Plasma has also been used for coating titanium alloy parts with hydroxyapatite [11, 12, 26] or different polymers under low-pressure conditions, such as allylamine [27, 28] or ethylenediamine [29]. Plasma is

also used to perform plasma electrolytic oxidation to coat titanium parts immersed in electrolytic solutions with hard ceramic coatings, such as TiO_2 for titanium parts, which can be later coated with hydroxyapatite [30]. Atmospheric plasma has also proven to induce hydrophilicity by the creation of reactive radicals over titanium surface [23, 31].

However, most of the related references in the literature focus their work on the evaluation of these treatments on pure titanium surfaces, while the experience about their effect on titanium alloys is limited, in spite of their importance in the manufacturing of bone and dental implants (especially Ti6Al4V, a α - β -type titanium alloy with excellent mechanical properties which is used in about the 50% of the biomedical implants [32]).

In the present study, low-pressure oxygen plasma has been applied to Ti6Al4V as a proposal to increase its bioaffinity. In addition to this, a comparison with other simple chemical treatments previously analyzed for titanium surface modification (acid etching [33] and peroxide oxidation [34]) has been established in terms of surface chemical groups, topography, water contact angle and cell viability. The effect of the treatments on the release of vanadium ions has also been assessed. Metallic ions can be released from Ti6Al4V implants to the surrounding and remote tissues [35–37] with relevant clinical implications, as vanadium ions are able to increase the number of apoptotic cells [37, 38].

A comparison between the effect of plasma, oxidizing and etching treatments has not been found in the literature (neither for titanium alloys nor for pure titanium), and the results could be helpful to better understand the differences between chemical treatments and low-pressure plasma treatment on the effects on the surface properties of this alloy.

Materials and methods

Materials

Experiments were carried out using 8-mm-diameter disks and $20 \times 20 \text{ mm}^2$ squares of a 1.6-mm-thick sheet of titanium grade V (Ti6Al4V or titanium ASTM B 265) from Ti-Shop.com (a division of William Gregor Ltd.). The disks were used for the biological evaluation of the surfaces, while the squared samples were subjected to physicochemical analysis. These samples were obtained by laser cutting.

Hydrogen peroxide 30% v/v was supplied by Merck KGaA. Hydrochloric acid 37% was provided by VWR Chemicals. Sulfuric acid 98.5% was supplied by Brenntag. Pure acetone 99.6% was obtained from LabKem (a subdivision from Labbox supplies), and absolute ethanol 99.5% was obtained from Scharlau Chemicals. Oxygen for plasma treatment was obtained from AirProducts (reference Ultrapure Plus oxygen—X50S). Ringer solution for the vanadium release evaluation

was purchased from Hemofarm. The standard used for the calibration curve in the atomic absorption spectroscopy quantification of vanadium ions was NH_4VO_3 , vanadium ICP standard from Merck. The following cells and reagents were used for cell culture: human osteoblasts hFOB 1.19 (ATCC[®] CRL-11372[™]), 1:1 mixture of Ham's F12 medium and Dulbecco's modified Eagle's medium (DMEM) with L-glutamine 2.5 mM and without phenol red (Gibco), fetal bovine serum (FBS) (Biowest), trypsin-EDTA (Capricorn Scientific), Geneticin[™] Selective Antibiotic G418 Sulfate (Gibco), PBS (Biowest) and 3-(4,5-dimethylthiazol-2-yl)-2,5-diphenyltetrazolium bromide (MTT) (from VWR).

Methods

Physical and chemical treatments

All the samples were cleaned with ultrasound for 10 min in the following sequence: acetone, ethanol 70% and distilled water. After that, they were allowed to dry in a desiccator with silica for 48 h.

Plasma treatment was conducted in a Zepto low-pressure plasma chamber from Diener electronic, using pure oxygen as gas. This device operates at 40 kHz and at a maximum power of 100 W; samples were plasma-treated at 100 W for 10 min, with an O_2 pressure of 1.5 mbar.

The chemical treatments consisted in the immersion of the samples in different oxidizing or etching solutions. These solutions are listed below:

- H_2O_2 30% (v/v) for 24 h in dark
- SCA (sulfuric and hydrochloric acids) for 1 h at 60 °C; SCA is a solution of $\text{H}_2\text{SO}_4/\text{HCl}/\text{H}_2\text{O}$ at a 1/1/1 ratio in volume

Once the chemical treatment is finished, each disk was washed with distilled water and allowed to dry in the desiccator for 2 days.

Fourier transform infrared spectroscopy (FT-IR)

All parts were analyzed in a FT-IR Spectrum Two device from PerkinElmer under the specular reflectance mode. Tests were performed using the 80 Spec tool at 0 degrees of polarization in the range from 500 to 4000 cm^{-1} , at a resolution of 16 cm^{-1} . These analyses were carried out in triplicate.

Scanning electron microscopy (SEM)–energy-dispersive X-ray spectroscopy (EDX)

SEM analyses were performed in a HITACHI TM3030 device, provided with an EDX sensor. Pictures were

taken at 15 kV and magnification of 150–2000, while EDX tests were performed at 15 kV and magnification of 150× (working distance 9300 μm and filament current of 1850 mA).

X-ray diffraction (XRD) tests

X-ray diffraction (XRD) analysis was performed with an X-ray diffractometer (Bruker D8 Advance A25, with a Cu target, $\lambda = 0.154$ nm). The samples were scanned from 23 to 80°. The system was operated at 40 kV and a current of 30 mA.

Water contact angle measurements

The water contact angle was measured with a Powereach contact angle meter (from Shanghai Zhongchen Digital Technology). The volume of distilled water drop used for the measurements was 3 μl , and the images were treated with StreamPix software. The static contact angle of each drop was measured on its right and left sides, and the value for each drop is the mean value of both measurements. For each group of samples, ten drops were evaluated.

Analysis of the release of vanadium ions

The release of ions from Ti6Al4V has been an issue of remarkable importance in the development of prosthesis made of this material. Vanadium release could be modified because of the surface modifications proposed in this study because of the potential passivation or activation. This ion could have a potential toxic effect, and for this reason, an evaluation of the release of vanadium ions in simulated body fluid from the samples was performed. Three square-shaped samples from each group were subjected to a corrosion test in an electrochemical cell consisting of 3 electrodes: the Ti6Al4V disk, the saturated potassium chloride electrode (XR110 Radiometer Analytical[®]) and a platinum electrode. The fluid of the cell where the samples were immersed was Ringer solution (10 ml per sample). This solution is a simulated body fluid with 147.1 mmol Na^+ , 4.0 mmol K^+ , 2.25 mmol Ca^{2+} and 155.6 mmol Cl^- . In this cell, the voltage was regulated from -250 mV up to 250 mV with a rate of 60 mV/min. With this cycle, the release of vanadium from the surfaces is expected to be increased compared to the immersion of the samples in simulated body fluids for a defined period of time. After this test, the Ringer solution was collected and analyzed by atomic absorption spectroscopy (Varian AA 280Z Zeeman) to quantify the levels of vanadium in these samples.

Cell culture

Human osteoblasts (hFOB 1.19, from ATCC[®] CRL-11372TM) were used to evaluate the cell affinity of the different groups of samples. Cells were cultured using a blend of Ham's F12 medium and DMEM supplemented with 2.5 mM L-glutamine, FBS at 10% and 0.3 mg/ml of G-418 sulfate. Once the flask reached 80–90% confluency, the cells were trypsinized with Trypsin-EDTA (0.5%) and transferred to a new flask. They were allowed to reach again the same level of confluency, and then, they were detached to be used in the seeding of the Ti6Al4V samples.

Four disks were used as replicas of each treatment for the cell culture. These samples were sterilized with UV radiation for 30 min.

A 50- μ l drop containing 1000 cells were placed over the Ti6Al4V disks placed in a 24-well plate, which was then introduced in the incubator at 37 °C and 5% CO₂ for one hour. Each well was then completed to 1 ml with fresh media and left again in the incubator for the specified culturing time.

Cell viability evaluation and cell morphology observation

The MTT [3-(4,5-dimethylthiazol-2-yl)-2,5-diphenyltetrazolium bromide] assay was used to evaluate the viability of the samples at days 1, 3 and 5 of cell culture. To carry out this test, the samples were transferred to a new well plate where the MTT reagent was added at a concentration of 1 mg/l, and left in the incubator for 18 h. Afterward, DMSO was added to dissolve the formazan crystals, measuring the developed color 30 min later in a plate reader ELX800 Universal Microplate Reader (BIO-TEK INSTRUMENTS). The data obtained were blank-corrected, and the figures obtained from absorbance will serve as an indicator of viable cells adhered to the Ti6Al4V parts.

Three more replicas were used for the cell culture carried out for 5 days. These samples were used for SEM observation of the cell spreading and morphology. To do so, media was removed and parts were washed with PBS twice. Then, cells were fixed using 1 ml of formalin for 10 min, repeated twice. After this, cells were dehydrated using solutions of increased alcohol content for 10 min, twice: 10%, 20%, 30%, 50%, 70%, 90%, absolute ethanol. Parts were then allowed to dry, metallized in a Quorum technologies mini sputter coater SC7620 model, using an Au/Pd target with a cycle of 120 s and 18 mA of intensity. Afterward, the samples were observed under SEM microscopy (5 kV).

Statistical analysis

For all quantitative data, the Wilcoxon test was used to evaluate if there was a significant difference in the treated

Ti6Al4V samples compared to untreated ones ($p < 0.05$ for significant and $p < 0.01$ for highly significant statistical difference). The implementation of this statistical method was carried out with MATLAB 7.4 (2007) software (Math-Works). All figures in this paper show the mean values of the results for each group, and their standard deviations are represented with error bars.

Results and discussion

Fourier transform infrared spectroscopy (FT-IR)

FT-IR is commonly used for characterization of chemical groups existing over different substrates, and it has been demonstrated to be also useful for Ti6Al4V characterization [39, 40].

Figure 1 shows the FT-IR spectra for untreated and treated titanium alloy parts at 0° polarization, which was found the optimal one to highlight the differences among treatments. The most interesting regions are placed in the range between 400 and 800 cm^{-1} [36], which are attributed to Ti–O and Ti–O–Ti bonds, and the bands placed at 890–900 cm^{-1} [19], which correspond to hydroxyl groups.

The acid solution treatment presented a weak peak at 890–900 cm^{-1} that could reveal –OH groups. This band was attenuated in comparison with untreated titanium spectra. On the other hand, SCA parts did not show any peak at 400–800 cm^{-1} , which means titanium oxides are removed from the surface due to the acid etching.

Plasma-treated parts show a spectrum very similar to untreated ones, being only remarkable the presence of titanium oxides, as determined by the peak at around 500 cm^{-1} , although from FT-IR studies it cannot be said that the amount of oxygen bonded to the parts surface has changed.

The most important differences in FT-IR spectra with respect to the untreated parts are seen for the H₂O₂-treated parts, where a strong peak around 890–900 cm^{-1} can be observed; this corresponds to –OH groups, which are responsible for the increase in the O/Ti ratio found by EDX analysis. The shoulder found in all spectra around 3700–3600 cm^{-1} corresponds to stretching vibration of H₂O that was absorbed on the surface [41] in all samples during cleaned phase.

As a conclusion of FT-IR analysis, it is only noticeable the appearance of –OH groups due to the H₂O₂ treatment and the reduction of titanium oxides due to acid etching; for this last, no chlorides or sulfate groups are observed in the parts surface as a consequence of chemical reagents used (HCl and H₂SO₄). TiO₂ has demonstrated to show biological effects, mainly when it is found in a crystalline form [42], and that is the reason to focus on this group in the surface analysis of treated parts.

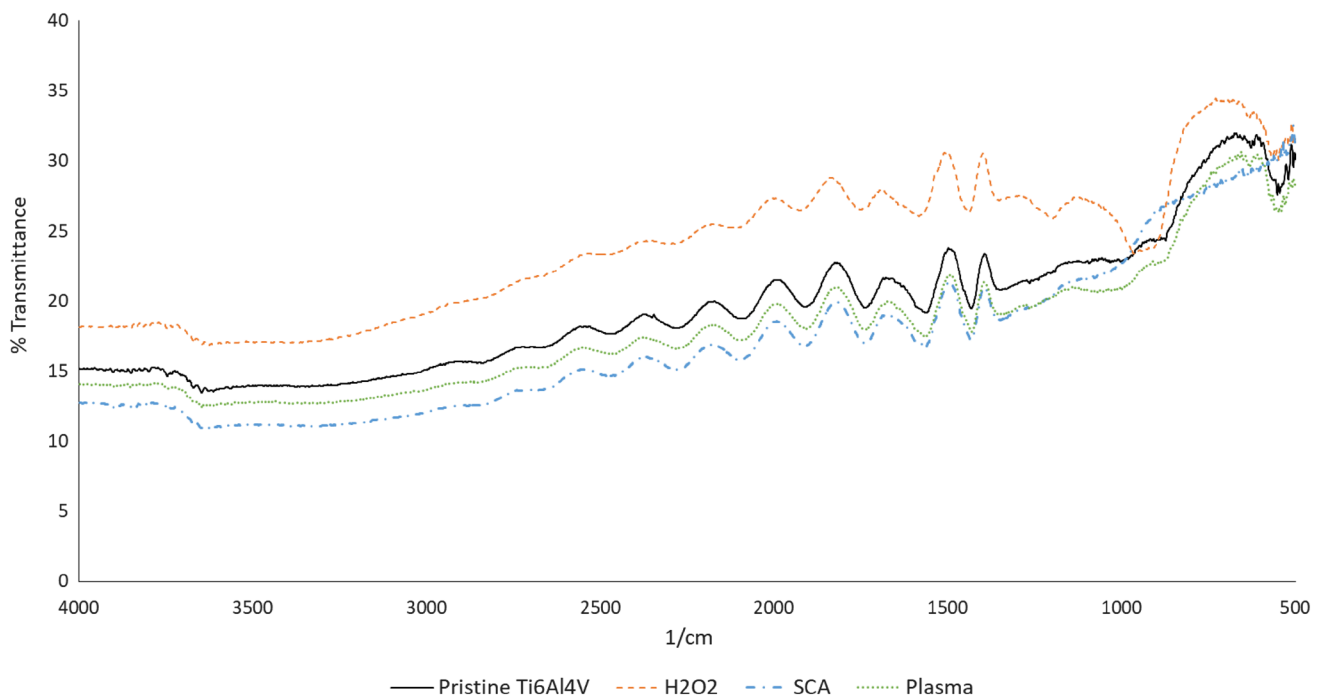


Fig. 1 Spectra for different Ti6Al4V treatments

Scanning electron microscopy (SEM)–energy-dispersive X-ray spectroscopy (EDX)

Figure 2 shows a comparison among different SEM pictures at the same condition for the different treatments applied. For untreated samples (Fig. 2a), anything else than some surface marks can be observed, while treated samples exhibit changes in surface topology. The plasma treatment scarcely affects the morphology of the surface of Ti6Al4V (Fig. 2b), which is in agreement with the results from Choi et al. [25], who reported that UV or non-thermal atmospheric pressure plasma jet does not affect the roughness of titanium grade IV samples. On the other hand, the H₂O₂ treatment (Fig. 2c) provides a relatively smooth surface with some heterogeneous points, where probably the oxidant treatment has been less aggressive because of local differences in composition on the original surface. Finally, SCA treatment (Fig. 2d) generates pores evenly distributed on the surface because of its etching effect.

Three samples per treatment were analyzed by EDX in order to determine surface composition of the parts and modifications induced due to the applied treatments. Table 1 provides the O/Ti ratios obtained for each type of sample, as average values.

From Table 1 it can be observed that acid treatment provides the lowest increase in the O/Ti ratio, while peroxide treatment maximizes this parameter, obtaining over than double of the initial value. Plasma treatment provides a

similar O/Ti ratio to untreated samples. (The difference represents 6% of the value for untreated samples, and it is not statistically significant $p > 0.05$.) For plasma-treated samples, different assays conducted show that oxygen content is higher just after plasma treatment (O/Ti = 0.44), but after 48 h at room temperature and humidity it does not show a remarkable change in terms of O/Ti ratio, as 6 days after the treatment the O/Ti is still similar to the mean value shown in Table 1 (0.35). However, a deeper analysis of the effect of aging on the properties of plasma-treated Ti6Al4V surfaces should be done in order to optimize the implementation of this procedure to the in vivo stage, as it could have an important impact on the biological performance of the parts.

As obtained from FT-IR analysis, which signaled a higher presence of titanium oxides over the surface of parts treated with H₂O₂, O/Ti ratio is higher for this treatment. (The difference is 117% of the value compared to untreated Ti6Al4V samples.)

Regarding these data, it can be stated that the smoother surface observed for the H₂O₂-treated samples (Fig. 2c) can be justified by the filling of the irregularities in untreated Ti6Al4V by the oxides generated and evidenced by elemental composition analysis and FT-IR evaluation.

X-ray diffraction (XRD) tests

EDX elemental composition data in Table 1 do not allow identifying the type of oxides that have been formed on

Fig. 2 SEM pictures for different surface treatments: pristine Ti6Al4V, plasma, H₂O₂ and SCA at 2000× magnification (scale bar: 30 μm)

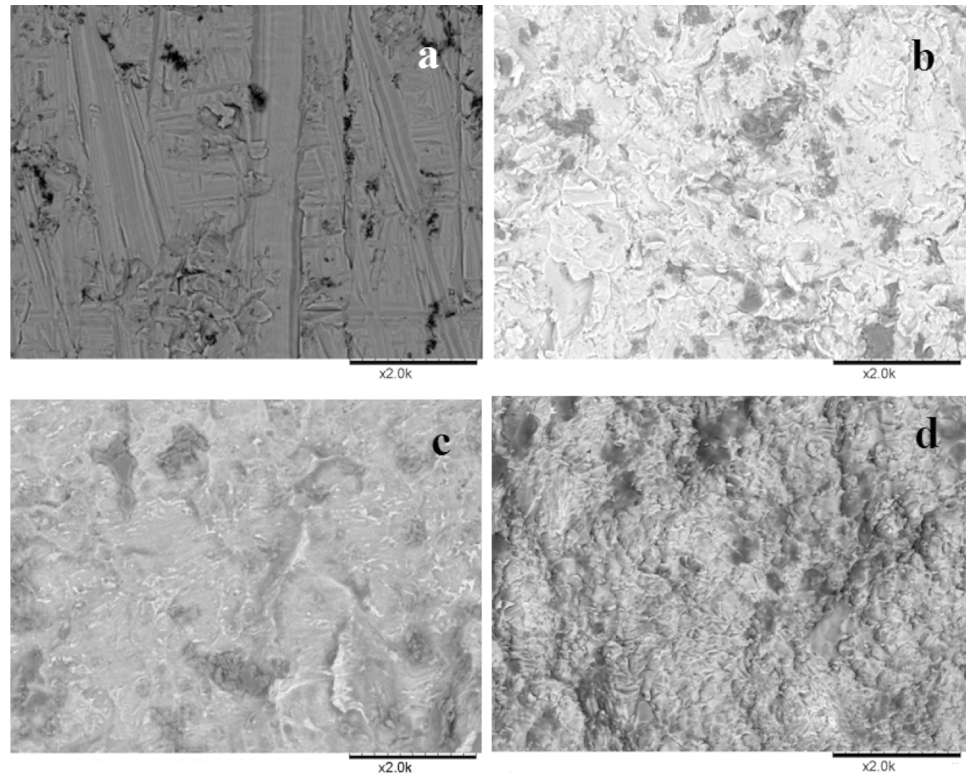


Table 1 O/Ti ratio for the different treatments obtained from EDX assays

Treatment	O/Ti (wt/wt)
Untreated	0.35 ± 0.11
Plasma	0.37 ± 0.05
H ₂ O ₂	0.76 ± 0.08**
SCA	0.32 ± 0.03

the surface, so XRD has been used to compare the relative formation of titanium oxides for the different surface treatments proposed in this study. Figure 3 shows the patterns for untreated Ti6Al4V and treated samples. All the patterns show the characteristic peaks of titanium at 35, 38 and 53° values of 2θ [43]. Titanium in Ti6Al4V alloys is a two-phase material (α and β) [44], and during acid etching (such as SCA treatment), both phases are attacked in a different way [35]. For this reason, it is possible to observe in the SCA-treated samples a modification in the relative intensities of the Ti peaks.

On the other hand, the peak at $2\theta = 57^\circ$ can be identified as one of the characteristic signals in the XRD pattern of rutile [36]. In Table 2, it is possible to observe the values of area of this peak for the patterns corresponding to each type of Ti6Al4V surface. These values show an increase in the signal for samples treated by plasma and by immersion in H₂O₂, but a decrease for the samples treated with SCA compared to the value for pristine Ti6Al4V. This decrease

can be justified by the reaction between the natural occurring TiO₂ layer on Ti6Al4V and the sulfuric acid in SCA solution [45]. On the other hand, the increase in the value for plasma and peroxide treatments can be explained by the formation of TiO₂ in the rutile phase during the procedure. These results are in agreement with the values for the O/Ti ratio obtained by EDX analysis (Table 1) and FT-IR (Fig. 1).

Water contact angle measurement

Table 3 shows the measurements of the water contact angle for the treated and untreated samples. There is a highly significant decrease in this parameter for the plasma-treated samples, compared to the untreated ones. On the other hand, SCA-treated samples were superhydrophilic and, therefore, it was not possible to carry out the measurement of their water contact angle (see supplementary material). This behavior can be explained by the morphology of the surface shown in Fig. 2d. Finally, H₂O₂ samples are slightly more hydrophilic than untreated ones, although this difference is not statistically significant.

Analysis of the release of vanadium ions

The concentration of vanadium in the Ringer solution samples coming from the evaluation of untreated Ti6Al4V is 66 ppb, the value of this parameter is 31 ppb for hydrogen

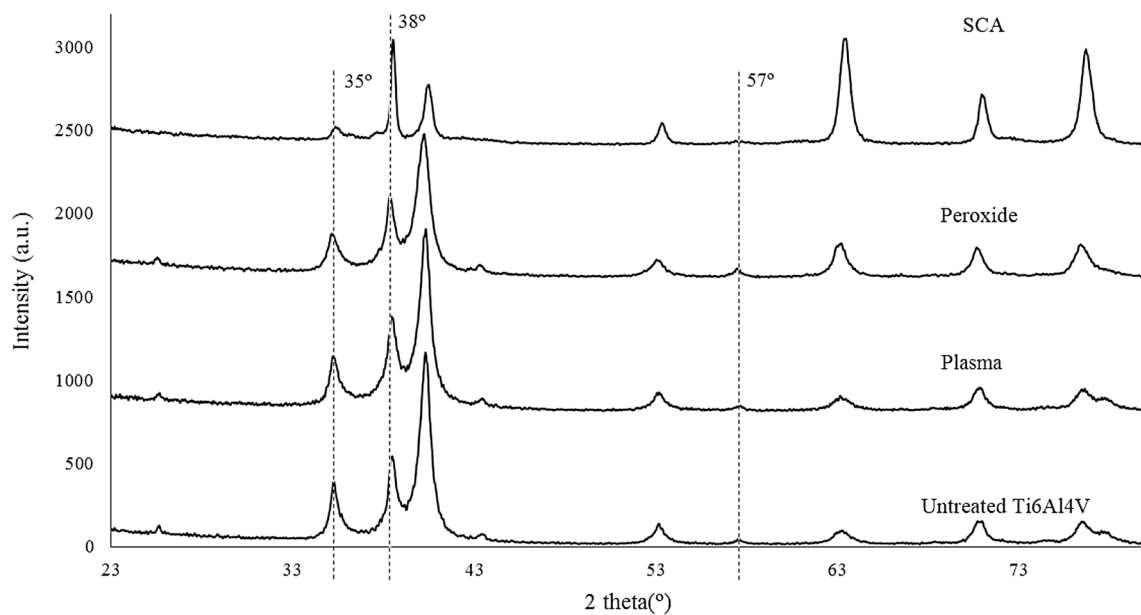


Fig. 3 XRD patterns for all the analyzed samples

Table 2 Area of the rutile peaks at $2\theta=57^\circ$ in the XRD patterns (calculated from raw data)

Treatment	Area of 2θ 57° peak
Untreated	545
Plasma	900
H ₂ O ₂	1500
SCA	464

Table 3 Water contact angle of treated and untreated Ti6Al4V samples (** $p < 0.01$ compared to pristine Ti6Al4V samples)

Treatment	Water contact angle
Untreated	101.98 ± 10.54
H ₂ O ₂	100.10 ± 6.65
Plasma	$76.34 \pm 7.40^{**}$
SCA	N/A

peroxide-treated samples, 63 ppb for plasma-treated ones and 45 ppb for the group treated with SCA. Hallab et al. [46] reported values of vanadium in the joint capsule of 122 ppb for control patients, 288 ppb for patients with well-functioning total joint arthroplasty and 1514 ppb for patients with poorly functioning total joint arthroplasty. As the highest values of released metallic ions can be found joint capsule, these values are a useful reference for the concentration values expected in the surrounding liquid to a Ti6Al4V implant, as the in vitro testing carried out during this study aimed to simulate this environment in an accelerated way. However, it is important to notice that those values reported in the literature from in vivo sampling and the ones provided in this paper from in vitro testing cannot be directly

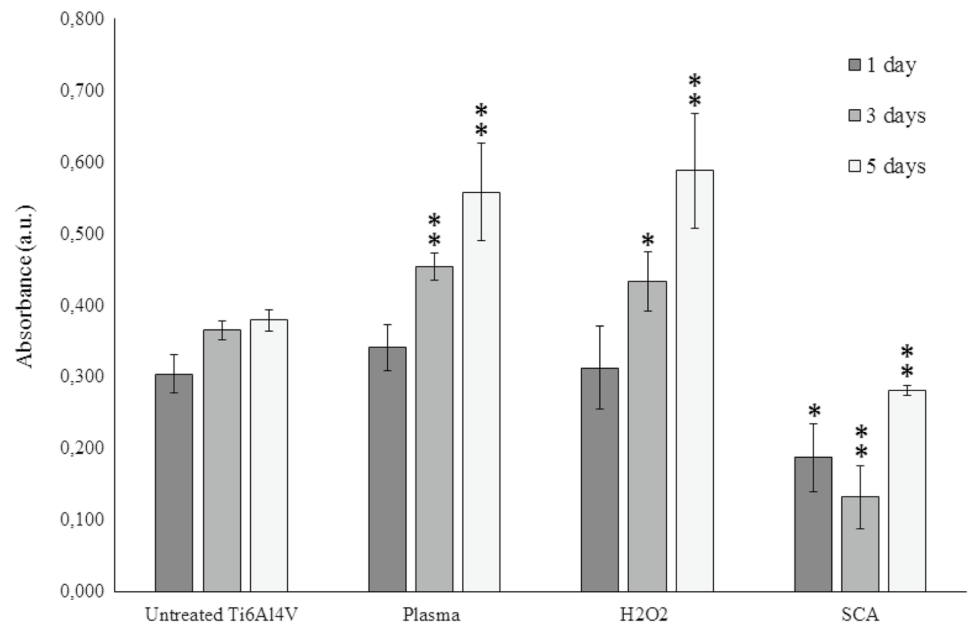
correlated. Nevertheless, these results are useful to evaluate if the oxides created during the treatments enhance or hinder the release of vanadium ions from the material with the clinical implications associated with this phenomenon. Regarding this issue, it is possible to conclude that none of the treatments enhances the vanadium release compared to the untreated Ti6Al4V group of samples, as the highest concentration value was found for this blank group.

The passivation layer on Ti6Al4V plays a crucial role in the corrosion processes [37] and, as a consequence, on the release of metallic ions. According to the XRD and elemental composition data previously shown, the surface treatment that provides a higher level of oxidation is the hydrogen peroxide one, as the rutile peak area in the XRD evaluation and the O/Ti in the EDX elemental analysis are the highest among the groups. This TiO₂ layer limits the vanadium release as evidenced by the data provided in the present study.

Cell viability evaluation and cell morphology observation

The MTT absorbance values (Fig. 4) show an increase in cell proliferation for H₂O₂- and plasma-treated samples, while there is a significant decrease in cell attachment for the SCA-treated samples. Similarly to the trend described by Aita et al. [21] the cell attachment does not correlate with the hydrophilicity of the surface, as the most hydrophilic group of samples (Table 3) shows the lowest cell affinity. This lack of cell attachment on the superhydrophilic surface of SCA-treated samples could be explained by a poorer adsorption

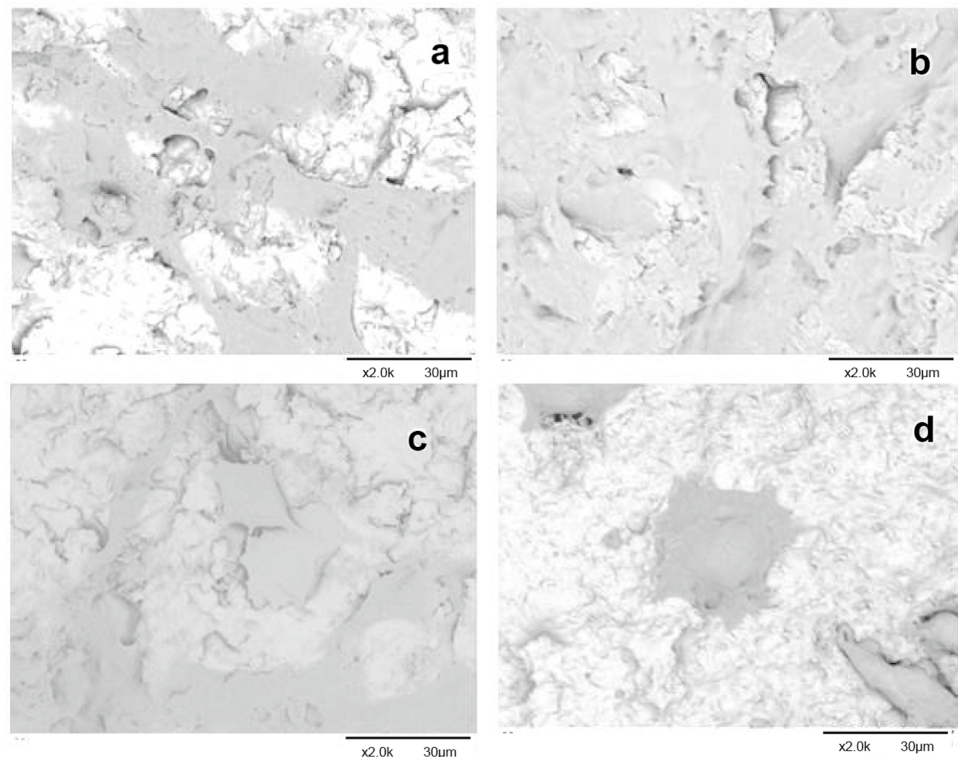
Fig. 4 Absorbance obtained on days 1, 3 and 5 for the different treatments ($*p < 0,05$ and $**p < 0,01$ compared to the group of pristine Ti6Al4V)



of adhesion-signaling extracellular proteins [47]. These serum proteins involved in cell adhesion can be absorbed on both hydrophilic and hydrophobic surfaces because of their amphiphilic character. However, depending on the wettability of the surface, the conformation they adopt can be modified [48]. Because of this behavior, there is a maximum hydrophilicity that increases osteoblasts attachment and, therefore, superhydrophilicity can limit the underlying

cell attachment processes. On the other hand, there is no significant difference ($p > 0,05$) between plasma-treated and peroxide-treated samples in terms of MTT absorbance. The samples treated with peroxide show an increased rutile peak in the XRD pattern (Table 2) and a higher O/Ti ratio on the surface (Table 1). These data point out a higher level of oxides. However, the contact angle is lower for plasma-treated samples. As both treatments are equivalent in terms

Fig. 5 SEM pictures for different surface treatments: **a** pristine Ti6Al4V, **b** H₂O₂, **c** plasma and **d** SCA at 2000× magnification. Scale bar: 30 μm



of in vitro cell attachment and spreading, it is possible to conclude that both surfaces have physicochemical characteristics that improve the affinity on the surface: one of them because of its chemical composition and the other one because of the change in the surface energy. Besides, it is important to highlight that further research is needed in order to take into account the effect of surface roughness on the modification of the biological properties of these samples due to the treatment.

On the other hand, as it is possible to observe in the pictures from SEM observation at day 5 of cell culture (Fig. 5), the cells develop more filopodia when they grow on plasma-treated and H₂O₂-treated surfaces than on pristine Ti6Al4V surfaces. Besides, the cell density that is observed in these pictures from SEM is consistent with the quantitative MTT data, as the surfaces in Fig. 5b, c (H₂O₂- and plasma-treated ones) show a more densely populated area than in Fig. 5a (pristine Ti6Al4V) and Fig. 5d (SCA-treated surface).

Conclusions

This study provides evidence of the suitability of low-pressure oxygen plasma as a treatment able to improve the cell affinity of Ti6Al4V surfaces. On the other hand, the comparison of results of this treatment with samples treated with conventional chemical procedures (oxidizing and acid etching) shows how the hydrophilicity is a key parameter during the cell attachment of human osteoblasts, as a parabolic correlation was found between the water contact angle and the MTT absorbance at Day 1 of the cell culture; hydrogen peroxide-treated parts show similar behavior in terms of cell adhesion, although surface characteristics (water contact angle and rutile content) are quite different. Due to the complexity of cell adhesion and spreading processes, further research is needed in order to deeper understand the role of each surface parameter in the biological behavior of Ti6Al4V surfaces.

Acknowledgements The authors would like to acknowledge the support of the Spanish Ministry of Economy and Competitiveness (MINECO), funding the SUPPORT project (DPI2015-71073-R) and the UNLP10-3E-726 Infrastructure Project (2010), co-financed with ERDF funds. M.E. Alemán would like to express her gratitude for the funding through the Ph.D. Grant Program of ULPGC (code of the Grant: PIFULPGC-2014-ING-ARQU-2) and the BAMOS project (H2020-MSCA-RISE-734156, funded from the European Union's Horizon 2020 research and innovation program) for providing funding for mobility.

Compliance with ethical standards

Conflict of interest Authors declare no conflict of interest.

Ethical approval This paper does not contain any studies with human or animal subjects.

References

1. Sandomierski M, Buchwald T, Strzemieska B, Voelkel A (2018) Modification of Ti6Al4V surface by diazonium compounds. *Spectrochim Acta Part A Mol Biomol Spectrosc* 191:27–35. <https://doi.org/10.1016/j.saa.2017.09.070>
2. Wang G, Fu H, Zhao Y, Zhou K, Zhu S (2017) Bone integration properties of antibacterial biomimetic porous titanium implants. *Trans Nonferrous Met Soc China* 27:2007–2014. [https://doi.org/10.1016/S1003-6326\(17\)60225-5](https://doi.org/10.1016/S1003-6326(17)60225-5)
3. Ataee A, Li Y, Fraser D, Song G, Wen C (2018) Anisotropic Ti–6Al–4V gyroid scaffolds manufactured by electron beam melting (EBM) for bone implant applications. *Mater Des* 137:345–354. <https://doi.org/10.1016/j.matdes.2017.10.040>
4. Hu X, Neoh KG, Shi Z, Kang ET, Poh C, Wang W (2010) An in vitro assessment of titanium functionalized with polysaccharides conjugated with vascular endothelial growth factor for enhanced osseointegration and inhibition of bacterial adhesion. *Biomaterials* 31:8854–8863. <https://doi.org/10.1016/j.biomaterials.2010.08.006>
5. Zhao L, Hu Y, Xu D, Cai K (2014) Surface functionalization of titanium substrates with chitosan–lauric acid conjugate to enhance osteoblasts functions and inhibit bacteria adhesion. *Colloids Surf B Biointerfaces* 119:115–125. <https://doi.org/10.1016/J.COLSURF.B.2014.05.002>
6. Osmon DR, Berbari EF, Berendt AR, Lew D, Zimmerli W, Steckelberg JM, Rao N, Hanssen A, Wilson WR (2013) Diagnosis and management of prosthetic joint infection: clinical practice guidelines by the infectious diseases Society of America. *Clin Infect Dis* 56:e1–e25. <https://doi.org/10.1093/cid/cis803>
7. Ahuir-Torres JL, Arenas MA, Perrie W, de Damborenea J (2018) Influence of laser parameters in surface texturing of Ti6Al4V and AA2024-T3 alloys. *Opt Lasers Eng* 103:100–109. <https://doi.org/10.1016/j.optlaseng.2017.12.004>
8. Moon B-S, Kim S, Kim H-E, Jang T-S (2017) Hierarchical micro-nano structured Ti6Al4V surface topography via two-step etching process for enhanced hydrophilicity and osteoblastic responses. *Mater Sci Eng C* 73:90–98. <https://doi.org/10.1016/j.msec.2016.12.064>
9. Ramskogler C, Warchomicka F, Mostofi S, Weinberg A, Sommitsch C (2017) Innovative surface modification of Ti6Al4V alloy by electron beam technique for biomedical application. *Mater Sci Eng C* 78:105–113
10. Habibovic P, Li J, van der Valk CM, Meijer G, Layrolle P, van Blitterswijk CA, de Groot K (2005) Biological performance of uncoated and octacalcium phosphate-coated Ti6Al4V. *Biomaterials* 26:23–36. <https://doi.org/10.1016/j.biomaterials.2004.02.026>
11. Stoch A, Jastrzębski W, Brozek A, Stoch J, Szaraniec J, Trybalska B, Kmita G (2000) FTIR absorption-reflection study of biomimetic growth of phosphates on titanium implants. *J Mol Struct*. [https://doi.org/10.1016/S0022-2860\(00\)00623-2](https://doi.org/10.1016/S0022-2860(00)00623-2)
12. Singh G, Singh S, Prakash S (2011) Surface characterization of plasma sprayed pure and reinforced hydroxyapatite coating on Ti6Al4V alloy. *Surf Coat Technol* 205:4814–4820. <https://doi.org/10.1016/j.surfcoat.2011.04.064>
13. He D, Liu P, Liu X, Ma F, Chen X, Li W, Du J, Wang P, Zhao J (2016) Characterization of hydroxyapatite coatings deposited by hydrothermal electrochemical method on NaOH immersed Ti6Al4V. *J Alloys Compd* 672:336–343. <https://doi.org/10.1016/j.jallcom.2016.02.173>

14. Jang CH, Lee H, Kim M, Kim GH (2018) Accelerated osteointegration of the titanium-implant coated with biocomponents, collagen/hydroxyapatite/bone morphogenetic protein-2, for bone-anchored hearing aid. *J Ind Eng Chem*. <https://doi.org/10.1016/j.jiec.2018.02.019>
15. Rodriguez GM, Bowen J, Grossin D, Ben-Nissan B, Stamboulis A (2017) Functionalisation of Ti6Al4V and hydroxyapatite surfaces with combined peptides based on KKLPGA and EEEEEEEE peptides. *Colloids Surf B Biointerfaces* 160:154–160. <https://doi.org/10.1016/j.colsurfb.2017.09.022>
16. Felgueiras HP, Migonney V (2016) Cell spreading and morphology variations as a result of protein adsorption and bioactive coating on Ti6Al4V surfaces. *IRBM* 37:165–171. <https://doi.org/10.1016/J.IRBM.2016.03.006>
17. Felgueiras HP, Decambon A, Manassero M, Tulasne L, Evans MDM, Viateau V, Migonney V (2017) Bone tissue response induced by bioactive polymer functionalized Ti6Al4V surfaces: in vitro and in vivo study. *J Colloid Interface Sci* 491:44–54. <https://doi.org/10.1016/j.jcis.2016.12.023>
18. Rodríguez-Cano A, Cintas P, Fernández-Calderón MC, Pacha-Olivenza MÁ, Crespo L, Saldaña L, Vilaboa N, González-Martín ML, Babiano R (2013) Controlled silanization-amination reactions on the Ti6Al4V surface for biomedical applications. *Colloids Surf B Biointerfaces* 106:248–257. <https://doi.org/10.1016/j.colsurfb.2013.01.034>
19. Michiardi A, Hélyar G, Nguyen PCT, Gamble LJ, Anagnostou F, Castner DG, Migonney V (2010) Bioactive polymer grafting onto titanium alloy surfaces. *Acta Biomater* 6:667–675. <https://doi.org/10.1016/j.actbio.2009.08.043>
20. Lv H, Chen Z, Yang X, Cen L, Zhang X, Gao P (2014) Layer-by-layer self-assembly of minocycline-loaded chitosan/alginate multilayer on titanium substrates to inhibit biofilm formation. *J Dent* 42:1464–1472. <https://doi.org/10.1016/j.jdent.2014.06.003>
21. Aita H, Hori N, Takeuchi M, Suzuki T, Yamada M, Anpo M, Ogawa T (2009) The effect of ultraviolet functionalization of titanium on integration with bone. *Biomaterials* 30:1015–1025. <https://doi.org/10.1016/j.biomaterials.2008.11.004>
22. Ueno T, Yamada M, Suzuki T, Minamikawa H, Sato N, Hori N, Takeuchi K, Hattori M, Ogawa T (2010) Enhancement of bone-titanium integration profile with UV-photofunctionalized titanium in a gap healing model. *Biomaterials* 31:1546–1557. <https://doi.org/10.1016/J.BIOMATERIALS.2009.11.018>
23. Lee J-H, Jeong W-S, Seo S-J, Kim H-W, Kim K-N, Choi E-H, Kim K-M (2017) Non-thermal atmospheric pressure plasma functionalized dental implant for enhancement of bacterial resistance and osseointegration. *Dent Mater* 33:257–270. <https://doi.org/10.1016/J.DENTAL.2016.11.011>
24. de Queiroz JDF, de Souza Leal AM, Terada M, Agnez-Lima LF, Costa I, de Souza Pinto NC, Batistuzzo de Medeiros SR (2014) Surface modification by argon plasma treatment improves antioxidant defense ability of CHO-k1 cells on titanium surfaces. *Toxicol Vitro* 28(2014):381–387. <https://doi.org/10.1016/j.tiv.2013.11.012>
25. Choi S-H, Jeong W-S, Cha J-Y, Lee J-H, Yu H-S, Choi E-H, Kim K-M, Hwang C-J (2016) Time-dependent effects of ultraviolet and nonthermal atmospheric pressure plasma on the biological activity of titanium. *Sci Rep* 6:33421. <https://doi.org/10.1038/srep33421>
26. Zreiqat H, Valenzuela SM, Ben Nissan B, Roest R, Knabe C, Radlanski RJ, Renz H, Evans PJ (2005) The effect of surface chemistry modification of titanium alloy on signalling pathways in human osteoblasts. *Biomaterials* 26:7579–7586. <https://doi.org/10.1016/j.biomaterials.2005.05.024>
27. Chen S, Usta AD, Eriten M (2017) Microstructure and wear resistance of Ti6Al4V surfaces processed by pulsed laser. *Surf Coat Technol* 315:220–231. <https://doi.org/10.1016/j.surfcoat.2017.02.031>
28. Rebl H, Finke B, Lange R, Weltmann KD, Nebe JB (2012) Impact of plasma chemistry versus titanium surface topography on osteoblast orientation. *Acta Biomater* 8:3840–3851. <https://doi.org/10.1016/j.actbio.2012.06.015>
29. Finke B, Hempel F, Testrich H, Artemenko A, Rebl H, Kylián O, Meichsner J, Biederman H, Nebe B, Weltmann KD, Schröder K (2011) Plasma processes for cell-adhesive titanium surfaces based on nitrogen-containing coatings. *Surf Coat Technol* 205:S520–S524. <https://doi.org/10.1016/j.surfcoat.2010.12.044>
30. Durdu S, Usta M, Berkem AS (2016) Bioactive coatings on Ti6Al4V alloy formed by plasma electrolytic oxidation. *Surf Coat Technol* 301:85–93. <https://doi.org/10.1016/j.surfcoat.2015.07.053>
31. Mussano F, Genova T, Verga Falzacappa E, Scopece P, Munaron L, Rivolo P, Mandracci P, Benedetti A, Carossa S, Patelli A (2017) In vitro characterization of two different atmospheric plasma jet chemical functionalizations of titanium surfaces. *Appl Surf Sci* 409:314–324. <https://doi.org/10.1016/j.apsusc.2017.02.035>
32. Cvijović-Alagić I, Cvijović Z, Bajat J, Rakin M (2016) Electrochemical behaviour of Ti-6Al-4V alloy with different microstructures in a simulated bio-environment. *Mater Corros* 67:1075–1087. <https://doi.org/10.1002/maco.201508796>
33. Kokubo T, Yamaguchi S (2016) Novel bioactive materials developed by simulated body fluid evaluation: surface-modified Ti metal and its alloys. *Acta Biomater* 44:16–30. <https://doi.org/10.1016/j.actbio.2016.08.013>
34. Daw AE, Kazi HAA, Colombo JS, Rowe WG, Williams DW, Waddington RJ, Thomas DW, Moseley R (2013) Differential cellular and microbial responses to nano-/micron-scale titanium surface roughness induced by hydrogen peroxide treatment. *J Biomater Appl* 28:144–160. <https://doi.org/10.1177/0885328212441495>
35. de Moraes LS, Serra GG, Albuquerque Palermo EF, Andrade LR, Müller CA, Meyers MA, Elias CN (2009) Systemic levels of metallic ions released from orthodontic mini-implants. *Am J Orthod Dentofac Orthop* 135:522–529. <https://doi.org/10.1016/j.ajodo.2007.04.045>
36. Chassot E, Irigaray J, Terver S, Vanneville G (2004) Contamination by metallic elements released from joint prostheses. *Med Eng Phys* 26:193–199. <https://doi.org/10.1016/J.MEDENGINPHYS.2003.10.008>
37. Costa BC, Tokuhara CK, Rocha LA, Oliveira RC, Lisboa-Filho PN, Costa Pessoa J (2018) Vanadium ionic species from degradation of Ti-6Al-4V metallic implants: in vitro cytotoxicity and speciation evaluation. *Mater Sci Eng C* 96:730–739. <https://doi.org/10.1016/j.msec.2018.11.090>
38. Montiel-Dávalos A, Gonzalez-Villava A, Rodriguez-Lara V, Montaña LF, Fortoul TI, López-Marure R (2012) Vanadium pentoxide induces activation and death of endothelial cells. *J Appl Toxicol* 32:26–33. <https://doi.org/10.1002/jat.1695>
39. Sharan J, Koul V, Dinda AK, Kharbanda OP, Lale SV, Duggal R, Mishra M, Gupta G, Singh MP (2018) Bio-functionalization of grade V titanium alloy with type I human collagen for enhancing and promoting human periodontal fibroblast cell adhesion—an in vitro study. *Colloids Surf B Biointerfaces* 161:1–9. <https://doi.org/10.1016/J.COLSURFB.2017.10.024>
40. Mamaghani AH, Haghighat F, Lee C-S (2018) Gas phase adsorption of volatile organic compounds onto titanium dioxide photocatalysts. *Chem Eng J* 337:60–73. <https://doi.org/10.1016/J.CEJ.2017.12.082>
41. Gomathi Thanga Keerthana B, Solaiyammal T, Muniyappan S, Murugakoothan P (2018) Hydrothermal synthesis and characterization of TiO₂ nanostructures prepared using different solvents. *Mater Lett* 220:20–23. <https://doi.org/10.1016/j.matlet.2018.02.119>

42. Mandracci P, Mussano F, Rivolo P, Carossa S (2016) Surface treatments and functional coatings for biocompatibility improvement and bacterial adhesion reduction in dental implantology. *Coatings* 6:7. <https://doi.org/10.3390/coatings6010007>
43. Chen YK, Ji H, Zheng XB (2007) Apatite formation on vacuum plasma sprayed titanium coating after chemical modification. In: *Thermal spray 2007: global coating solutions*. ASM International. https://www.asminternational.org/home/-/journal_content/56/10192/CP2007ITSC0381/CONFERENCE-PAPER
44. Li R, Riestler L, Watkins TR, Blau PJ, Shih AJ (2008) Metallurgical analysis and nanoindentation characterization of Ti–6Al–4V workpiece and chips in high-throughput drilling. *Mater Sci Eng A* 472:115–124. <https://doi.org/10.1016/J.MSEA.2007.03.054>
45. Ban S, Iwaya Y, Kono H, Sato H (2006) Surface modification of titanium by etching in concentrated sulfuric acid. *Dent Mater* 22:1115–1120. <https://doi.org/10.1016/J.DENTAL.2005.09.007>
46. Hallab NJ, Mikecz K, Vermes C, Skipor A, Jacobs JJ (2001) Orthopaedic implant related metal toxicity in terms of human lymphocyte reactivity to metal-protein complexes produced from cobalt-base and titanium-base implant alloy degradation. *Mol Cell Biochem* 222:127–136. <https://doi.org/10.1023/A:1017979710992>
47. Alemán-Domínguez ME, Ortega Z, Benítez AN, Vilarriño-Feltrre G, Gómez-Tejedor JA, Vallés-Lluch A (2018) Tunability of polycaprolactone hydrophilicity by carboxymethyl cellulose loading. *J Appl Polym Sci* 135:46134. <https://doi.org/10.1002/app.46134>
48. Chen S, Guo Y, Liu R, Wu S, Fang J, Huang B, Li Z, Chen Z, Chen Z (2018) Tuning surface properties of bone biomaterials to manipulate osteoblastic cell adhesion and the signaling pathways for the enhancement of early osseointegration. *Colloids Surf B Biointerfaces* 164:58–69. <https://doi.org/10.1016/J.COLSU.2018.01.022>

Affiliations

María Elena Alemán-Domínguez¹ · Zaida Ortega¹  · Antonio N. Benítez¹ · Aday Romero-Pérez² · Ling Wang³ · Ruymán Santana-Farré² · Francisco Rodríguez-Esparragón⁴

¹ Departamento de Ingeniería de Procesos, Universidad de Las Palmas de Gran Canaria, Campus universitario de Tafira Baja, 35017 Las Palmas de Gran Canaria, Spain

² Departamento de Ingeniería Mecánica, Universidad de Las Palmas de Gran Canaria, Campus universitario de Tafira Baja, 35017 Las Palmas de Gran Canaria, Spain

³ State Key Laboratory for Manufacturing System Engineering, School of Mechanical Engineering, Xi'an Jiaotong University, Science and Technology Park of Xi'an Jiaotong University, Yanta District, Xi'an City 710054, Shaanxi Province, People's Republic of China

⁴ Research Unit, Dr. Negrín University Hospital, 35019 Las Palmas, Canary Islands, Spain